

Article

# Feasibility of a Reusable Radiochromic Dosimeter

Joseph R. Newton <sup>1,\*</sup>, Maxwell Recht <sup>1</sup>, Joseph A. Hauger <sup>1</sup>, Gabriel Segarra <sup>1</sup>, Chase Inglett <sup>1</sup>, Pedro A. Romo <sup>1</sup> and John Adamovics <sup>2</sup>

<sup>1</sup> Department of Chemistry and Physics, Augusta University, Augusta, GA 30912, USA; mreht@augusta.edu (M.R.); jhauger@augusta.edu (J.A.H.); gsegarra415@gmail.com (G.S.); cinglett23@gmail.com (C.I.); pedroaromo@outlook.com (P.A.R.)

<sup>2</sup> Department of Chemistry and Biochemistry, Rider University, Lawrenceville, NJ 08648, USA; jadamovics@rider.edu

\* Correspondence: JNEWTON3@augusta.edu

**Abstract:** The current practice for patient-specific quality assurance (QA) uses ion chambers or diode arrays primarily because of their ease of use and reliability. A standard routine compares the dose distribution measured in a phantom with the dose distribution calculated by the treatment planning system for the same experimental conditions. For the particular problems encountered in the treatment planning of complex radiotherapy techniques, such as small fields/segments and dynamic delivery systems, additional tests are required to verify the accuracy of dose calculations. The dose distribution verification should be throughout the total 3D dose distribution for a high dose gradient in a small, irradiated volume, instead of the standard practice of one to several planes with 2D radiochromic (GAFChromic) film. To address this issue, we have developed a 3D radiochromic dosimeter that improves the rigor of current QA techniques by providing high-resolution, complete 3D verification for a wide range of clinical applications. The dosimeter is composed of polyurethane, a radical initiator, and a leuco dye, which is radiolytically oxidized to a dye absorbing at 633 nm. Since this chemical dosimeter is single-use, it represents a significant expense. The purpose of this research is to develop a cost-effective reusable dosimeter formulation. Based on prior reusability studies, three promising dosimeter formulations were studied using small volume optical cuvettes and irradiated to known clinically relevant doses of 0.5–10 Gy. After irradiation, the change in optical density was measured in a spectrophotometer. All three formulations retained linearity of optical density response to radiation upon re-irradiations. However, only one formulation retained dose sensitivity upon at least five re-irradiations, making it ideal for further evaluation as a 3D dosimeter.

**Keywords:** radiation therapy verification; dosimetry; radiochromic; reusability



**Citation:** Newton, J.R.; Recht, M.; Hauger, J.A.; Segarra, G.; Inglett, C.; Romo, P.A.; Adamovics, J. Feasibility of a Reusable Radiochromic Dosimeter. *Appl. Sci.* **2021**, *11*, 9906. <https://doi.org/10.3390/app11219906>

Academic Editors: Cinzia Talamonti, Marco Petasecca and Simona Giordanengo

Received: 23 September 2021

Accepted: 18 October 2021

Published: 23 October 2021

**Publisher's Note:** MDPI stays neutral with regard to jurisdictional claims in published maps and institutional affiliations.



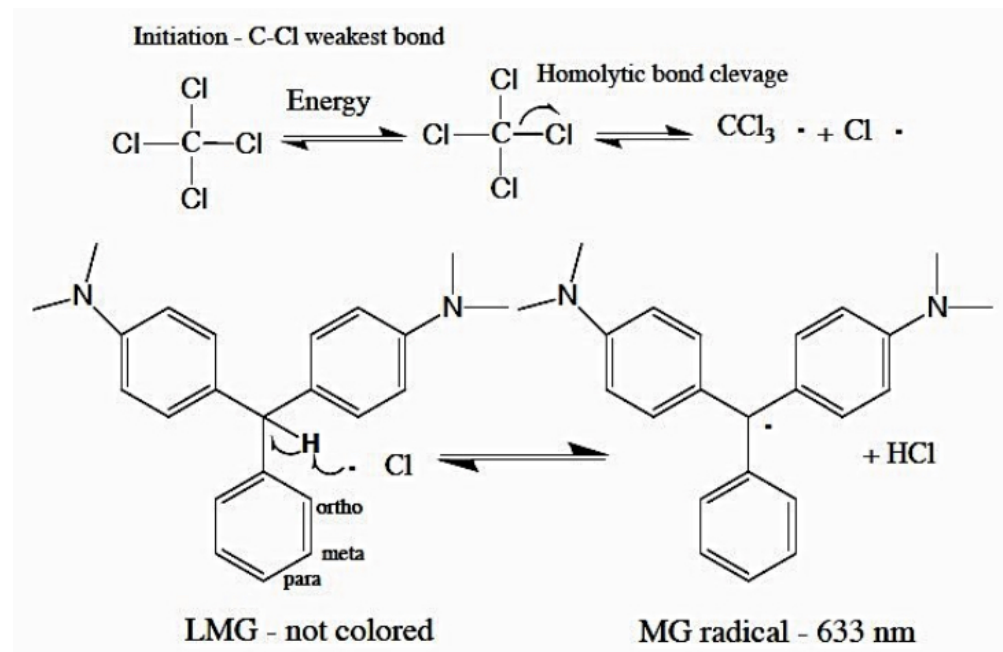
**Copyright:** © 2021 by the authors. Licensee MDPI, Basel, Switzerland. This article is an open access article distributed under the terms and conditions of the Creative Commons Attribution (CC BY) license (<https://creativecommons.org/licenses/by/4.0/>).

## 1. Introduction

For medical physics applications, the dosimetric properties of thermoluminescent dosimeters (TLD) and optically stimulated luminescent dosimeters (OSLD) have shown to be practical, accurate, and precise tools for point dosimetry [1]. An advantage of these inorganic-based detectors is that they are reusable after removing the original signal. The TLD signal is deleted by heating, while OSLDs are cleared by exposure to light. Two-dimensional (2D) thermoluminescence dosimeters are being developed but have not been widely accepted owing to their non-uniformity, low repeatability, and energy dependence [2]. The other formatted 2D dosimeters that have shown clinical applicability are silver halide-based x-ray film (radiographic film) and the more common Gafchromic<sup>®</sup> film containing a diacetylene (e.g., 10,12-pentacosadiynoic acid) active layer; neither format has post-irradiation reusable characteristics [3]. Potentially, a modified polydiacetylene film containing alkali metal salts may have reversible color-changing properties [4,5].

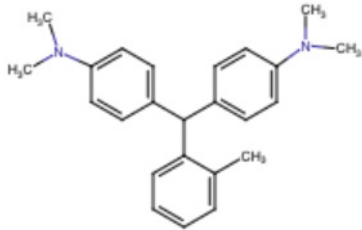
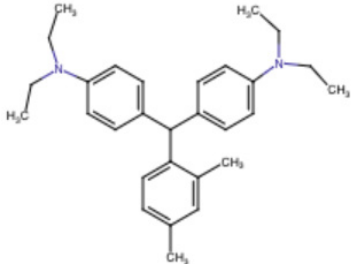
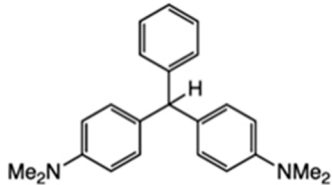
In contrast, reusability has been demonstrated in 2D radiochromic dosimeter sheets (3 mm thick) based on a PRESAGE<sup>®</sup> formulation [6] and confirmed to be usable after eight

irradiations. However, the PRESAGE<sup>®</sup> 2D formulation described by Collins is not scalable to the volumes required for fabricating a 3D dosimeter equivalent formulation due to heat degradation during the curing phase of the larger volumes (>1 kg). Therefore, this study aims to evaluate in small dosimeters (cuvettes) three additional PRESAGE<sup>®</sup> formulation components from prior studies [7–10] that are known to be stable at the scales used in 3D manufacturing. The primary components of PRESAGE formulations are a triarylmethane leuco dye (TAM) and a radical initiator with the preferred containing carbon halogen bonds. Mechanistically, radicals generated after irradiation with the most labile from the cleavage of the carbon chloride bond, which reacts with the next labile bond (methine bond, central carbon) in the TAM. This reaction creates a colored resonance stabilized free radical and HCl (e.g., ca. > 600 nm) (Figure 1). The chemical structures of numerous TAMs have been evaluated in 3D dosimeters [10,11]. The density of the TAM radical is primarily on the central carbon with some charge distribution to the nitrogen substituents [10,11]. Radical stability and sensitivity are primarily due to steric protection of the central carbon and to polar solvents such as dimethyl sulfoxide. These factors influence the equilibrium between the radical (colored TAM) and the colorless starting leuco dye. The three TAMs, along with their formulations, are shown in (Table 1). Structures 1 and 2 were chosen because the methine is structurally hindered, which is reflected in the post-irradiation color stability of over 500 h with 4% solvent in the formulation, while the color is bleached after 320 h when formulated with 15% solvent [10,11].



**Figure 1.** A mechanism for color formation in TAM (LMG) color former.

**Table 1.** Three formulations studied for reusability.

Formulation #	TAM Structure
1. 1.5%-Methyl-LMG-DMA; 0.4% CBr <sub>4</sub> Molecular Ratio TAM: CBr <sub>4</sub> (1:0.21)	
2. 1.5% 2,4 Dimethyl-LMG-DEA; 0.4% CBr <sub>4</sub> Molecular Ratio (1:0.4)	
3. 2% LMG; 1.5% CBr <sub>4</sub> Molecular Ratio (1:0.75)	

## 2. Materials and Methods

### 2.1. Materials

Table 1 describes the three formulations studied. First, a liquid precise aliphatic polyurethane formulation containing TAM and radical initiator were filled into standard plastic cuvettes 4.5 cm tall, 1 cm × 1 cm cross-section, then cured at room temperature under 60 psi pressure for 8 to 24 h. These small dosimeters were stored in lab storage drawers to avoid light exposure. Second, there were a sufficient number of Formulation 3 cuvettes manufactured to allow for two separate groups of cuvettes to be investigated independently. These will be referred to as Formulation 3 Groups 1 and 2.

### 2.2. Irradiation/Scanning of the Formulated Cuvettes

Each cuvette was irradiated at the Georgia Radiation Therapy Center (Augusta, Georgia) using 6 MV Clinac (Varian) photon beams. Doses ranged from 0.5, 1.0, 2.0, 4.0, 6.0, 8.0, 10 Gy with non-irradiated controls. The cuvettes were individually irradiated using a SAD (source-axis distance) set up at a depth of 4.6 cm in solid water with 5.0 cm of backscatter (Figure 2). The cuvettes were scanned with a spectrophotometer (Genesys 20 Thermo Spectronic). The change in OD across the width of the cuvette was calculated using the pre- and post-scans for a  $\Delta$ OD measurement. After scanning, the cuvettes were returned to a light-tight container and placed in a lab storage drawer. The cuvettes were then rescanned periodically, and after the optical density (OD) cleared to a stable baseline, the cuvettes were re-irradiated. The three dosimetric parameters evaluated were linearity, temporal sensitivity, and dose sensitivity response upon reirradiation.

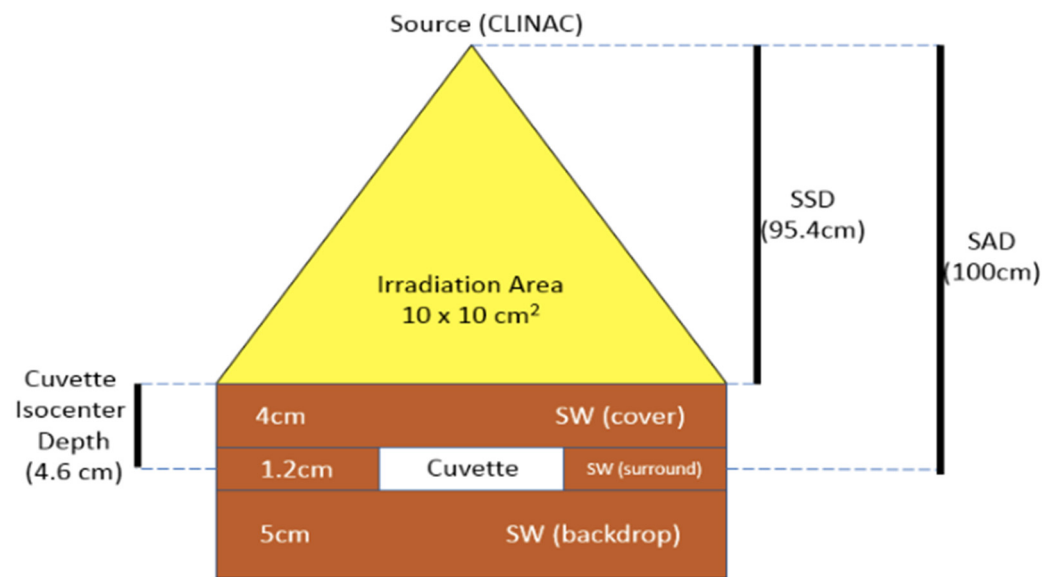


**Figure 2.** Cuvette irradiation setup. The cuvette was placed on top of a 5 cm thick backdrop of solid water and then surrounded by a solid water layer 1.2 cm thick. An additional 4.0 cm thick layer of solid water was then used to cover the cuvette. The center of the cuvette was moved to the isocenter at SAD = 100 cm. The SSD (source-surface distance) is set to 95.4 cm. The collimator field size is  $10.0 \times 10.0 \text{ cm}^2$ .

### 2.3. Dosimetric Evaluations

In evaluating the dosimeter's dose-response prediction accuracy with a linear regression model, metrics such as mean absolute percentage error (MAPE) and the coefficient of determination ( $R^2$ ) were used. MAPE describes the relative deviation that the measured  $\Delta OD$  has from its corresponding forecasted value at each dose and measurement time point over a given number of fitted data points. The forecasted values were acquired using a fitted linear trend line function derived from the plot of the measured  $\Delta OD$  values. The coefficient of determination ( $R^2$ ) describes how well the linear regression model fits the entire set of observations. The temporal stability of the three dosimeter formulations post-irradiation, the measured optical response ( $\Delta OD$ ), dose-response sensitivity ( $\Delta OD/\text{Gy}$ ), and linear dose-response of the dosimeter was considered. The 10 Gy cuvettes were chosen for clearing time analysis because they experienced the greatest range of OD clearing.

## 3. Results

### 3.1. Linearity of First Irradiation Response

The dose-responses upon first irradiation of all three formulations are plotted in Figure 3. Each data set is fit with a linear regression model, and the  $R^2$  coefficients are included.

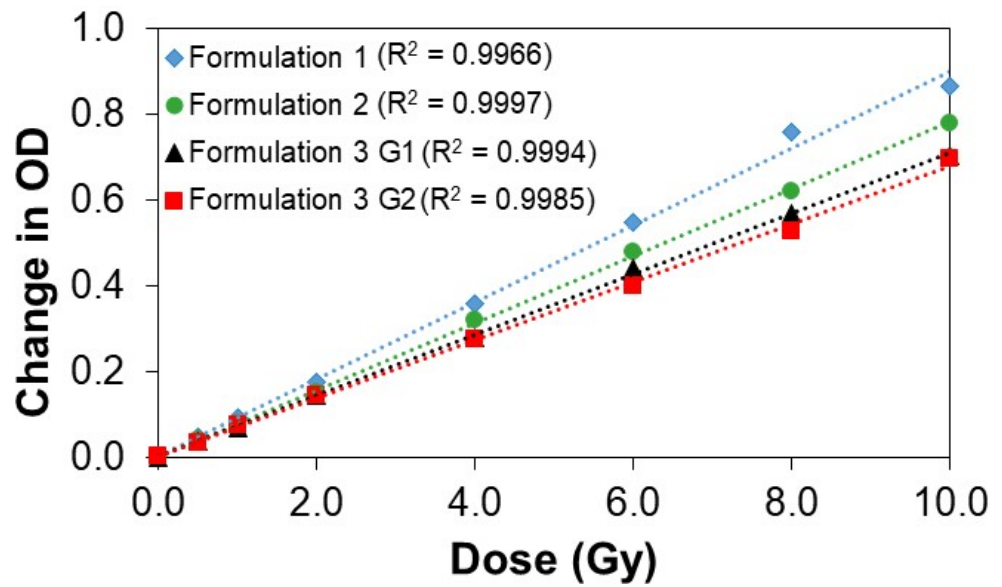


**Figure 3.** After the first irradiation, the initial cuvette dose response for Formulation 1, Formulation 2 and both groups of Formulation 3 (labeled G1 and G2 for group 1 and 2, respectively) are plotted above. Again, the least-squares linear fits are included as dotted lines along with the associated  $R^2$  coefficient of the fit.

### 3.2. Temporal Characteristics

The clearing data for initial irradiation of seven cuvettes of Formulation 1 (Figure 4), Formulation 2 (Figure 5), and Formulation 3 (Figure 6) are shown for all doses. The data were fit with an exponential decay curve to determine a time constant for the exponential decay. The fit equations are  $y = y_0 + Ae^{-\lambda t}$ , where  $A$  is the immediate post-irradiation OD and  $y_0$  is the decay baseline. The goal was not to determine a high precision time constant but rather to gain a general understanding of how long the cuvettes require to return to a stable baseline to be reused for dosimetry measurements.

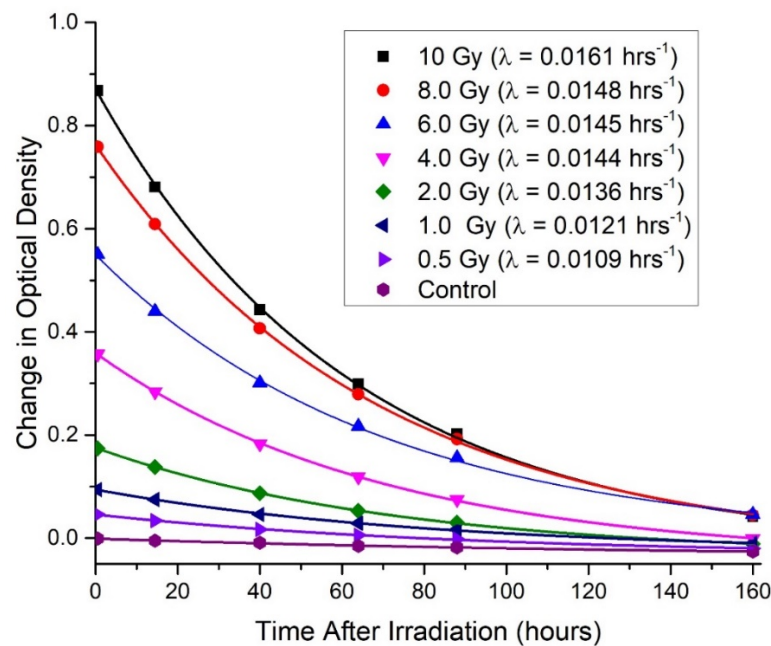


**Figure 4.** After initial irradiation, the clearing curves for the Formulation 1 cuvettes irradiated up to a maximum dose of 10 Gy were tracked for several days for all seven irradiated cuvettes. Fits to the curves were performed using a three-parameter fit function of the form  $y = y_0 + Ae^{-\lambda t}$ .

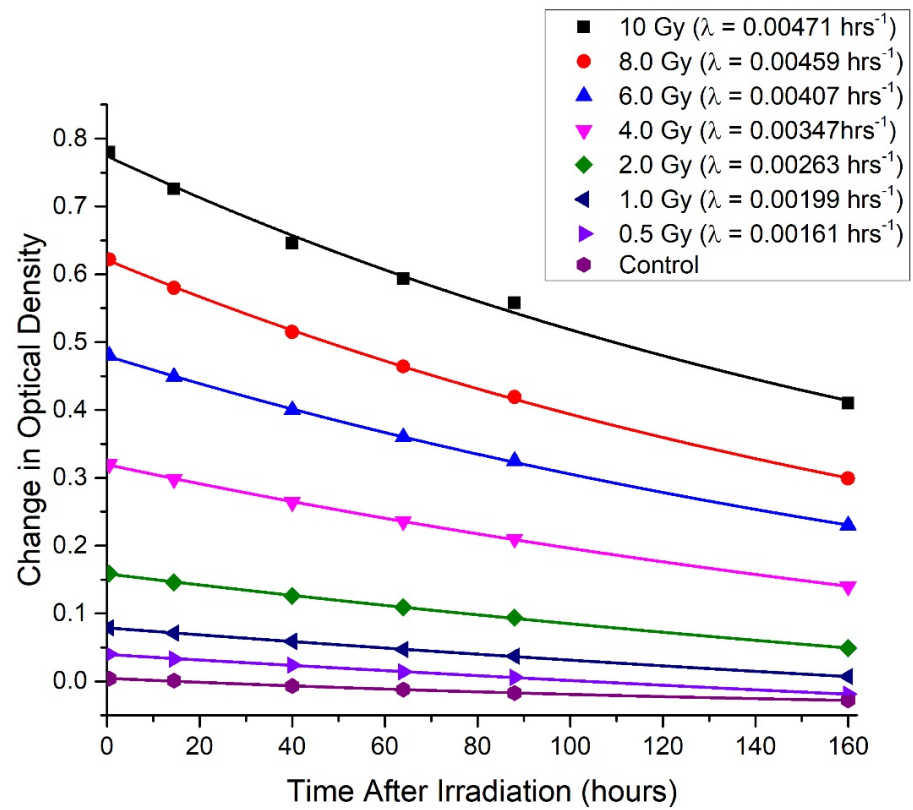


**Figure 5.** After initial irradiation, the clearing curves for the Formulation 2 cuvettes irradiated up to a maximum dose of 10 Gy were tracked for several days for all seven irradiated cuvettes. Fits to the curves were performed using a three-parameter fit function of the form  $y = y_0 + Ae^{-\lambda t}$ .

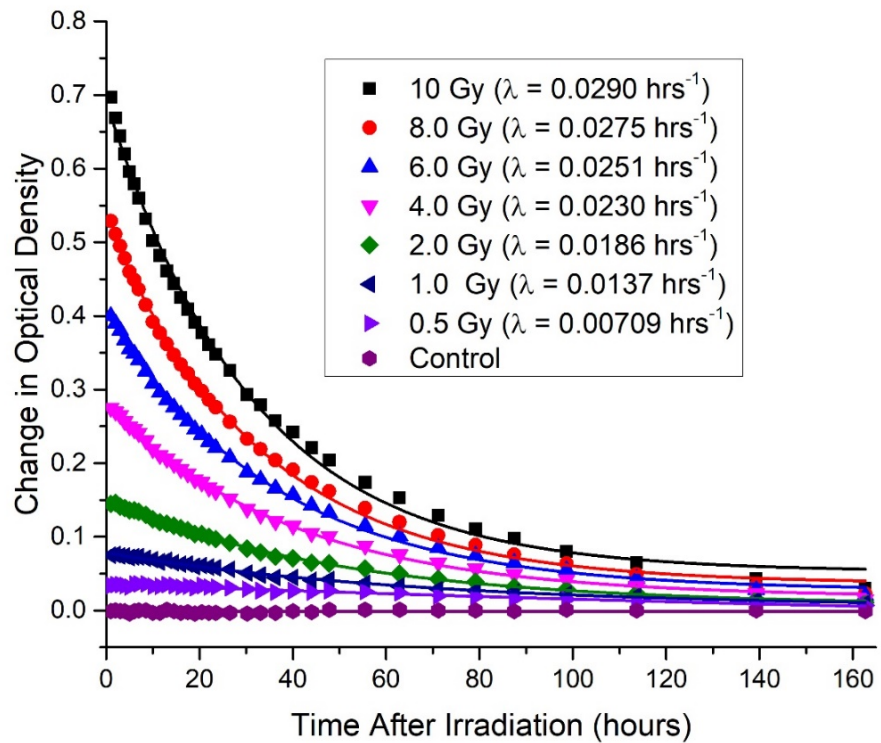


**Figure 6.** After initial irradiation, the clearing curves for the Formulation 3 cuvettes irradiated up to a maximum dose of 10 Gy were tracked for several days for all seven irradiated cuvettes. Fits to the curves were performed using a three-parameter fit function of the form  $y = y_0 + Ae^{-\lambda t}$ .



### 3.3. Reusability (Multiple Irradiations) Linearity and Dose Sensitivity

For purposes of reusability, only Formulation 1 and Formulation 3 will be further considered, as the slow clearing response of Formulation 2 is not ideal. This will be explained in detail in the discussion. The linearity data for Formulation 1 (Figure 7, Tables 2 and 3) are shown for each of the five irradiations. A positive correlation ranging from  $R^2 = 0.9966$  to  $0.9993$  was found for all linear fits.

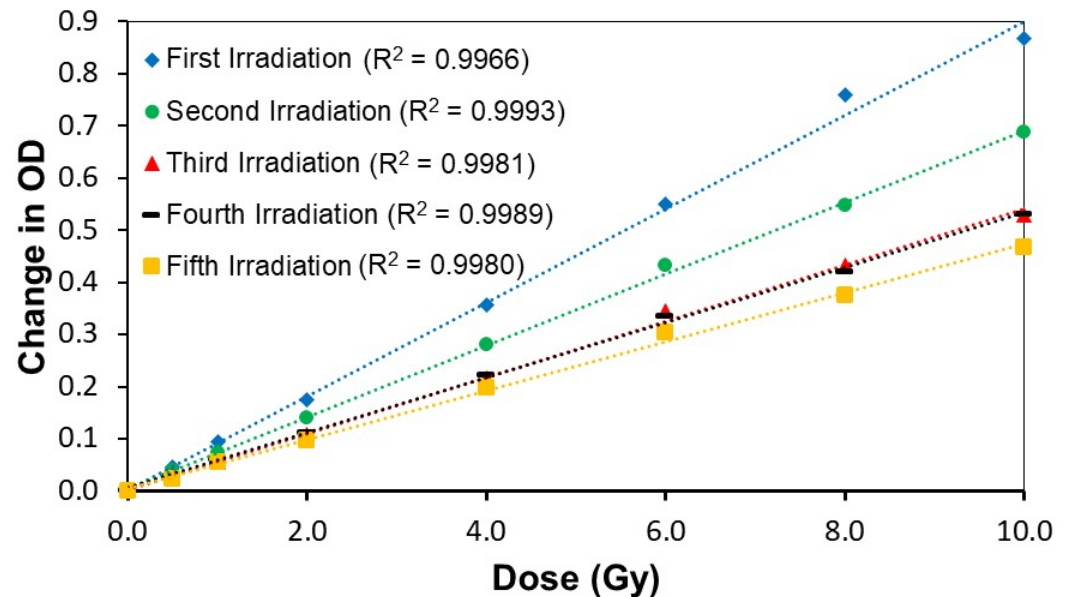


**Figure 7.** Five separate irradiations of Formulation 1 with seven cuvettes ranging from 0.5–10 Gy dose. The reirradiations were performed well after the cuvettes had cleared back to a stable baseline OD following the previous irradiation. Least squares linear fits to each of the five data sets are shown above, with the  $R^2$  coefficient included for each.

**Table 2.** Formulation 1 sensitivity measurements for five successive irradiations along with the percent change from the initial sensitivity.

Irradiation #	$\Delta OD/Gy$	% Change
First	0.0898	0
Second	0.0686	−23.6
Third	0.0538	−40.1
Fourth	0.0527	−41.3
Fifth	0.0469	−47.7

**Table 3.** Linearity values for Formulation 1 for five successive irradiations. The mean average percent error (MAPE) calculation includes cuvettes dosed with 1–10 Gy. The  $R^2$  coefficient of linearity is also included.

Irradiation #	MAPE %	Least Squares $R^2$
First	3.05	0.9966
Second	1.24	0.9993
Third	2.14	0.9981
Fourth	4.46	0.9989
Fifth	3.92	0.9980

The linearity data for two separate groups (designated Group 1 and Group2) of Formulation 3 cuvettes (Figures 8 and 9, Tables 4 and 5) are shown for each of the five irradiations of both groups, indicating a positive correlation ranging from  $R^2 = 0.9963$  to  $0.9994$  for all irradiations.

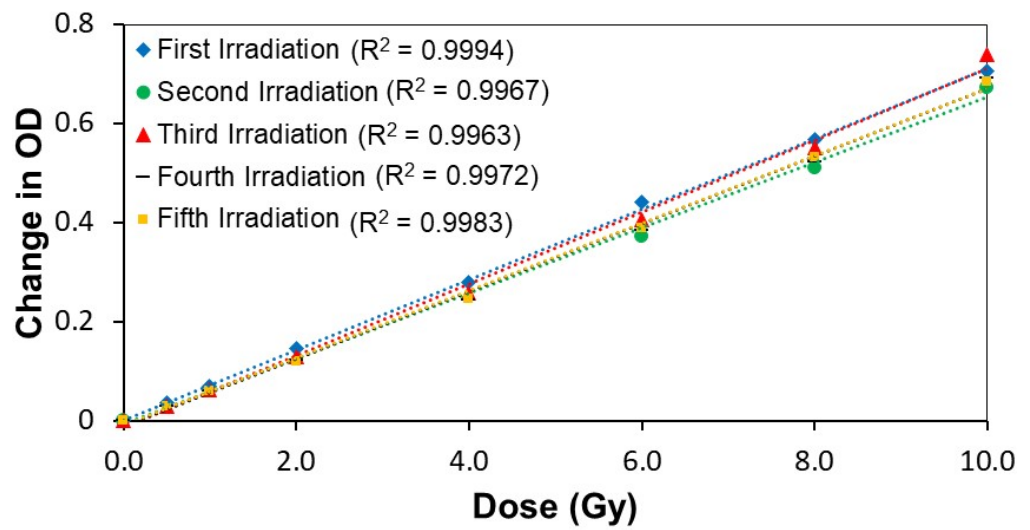


**Figure 8.** Five separate irradiations of Formulation 3 Group 1 with seven cuvettes ranging from 0.5–10 Gy dose. The reirradiations were performed well after the cuvettes had cleared back to a stable baseline OD following the previous irradiation. Least squares linear fits to each of the five data sets are shown above, with the  $R^2$  coefficient included for each.

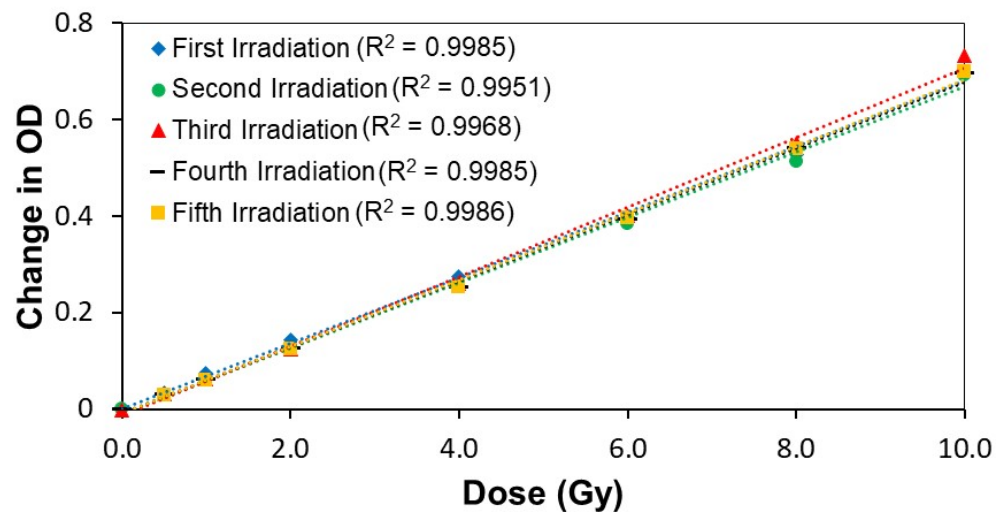


**Figure 9.** Five separate irradiations of Formulation 3 Group 2 with seven cuvettes ranging from 0.5–10 Gy dose. The reirradiations were performed well after the cuvettes had cleared back to a stable baseline OD following the previous irradiation. Least squares linear fits to each of the five data sets are shown above, with the  $R^2$  coefficient included for each.

**Table 4.** Formulation 3 (Groups 1 and 2) sensitivity measurements for five successive irradiations along with the percent change from the initial sensitivity.

Irradiation #	$\Delta OD/Gy$ Group 1	% Change	$\Delta OD/Gy$ Group 2	% Change
First	0.0710	0	0.0678	0
Second	0.0661	−6.9	0.0677	−1.5
Third	0.0723	1.8	0.0720	6.2
Fourth	0.0680	−4.2	0.0689	1.6
Fifth	0.0680	4.2	0.0693	2.2



**Table 5.** Linearity values for Formulation 3 (Groups 1 and 2) for five successive irradiations. The mean average percent error (MAPE) calculation includes cuvettes dosed with 1–10 Gy. The R<sup>2</sup> coefficient of linearity is also included.

Irradiation #	MAPE% Group 1	Least Squares R <sup>2</sup>	MAPE % Group 2	Least Squares R <sup>2</sup>
First	1.78	0.9994	3.23	0.9985
Second	4.68	0.9967	2.45	0.9951
Third	4.40	0.9963	4.22	0.9968
Fourth	3.79	0.9972	3.48	0.9985
Fifth	3.60	0.9983	2.87	0.9986

Figure 10 shows the measured sensitivity values of all five irradiations of Group 1 and Group 2 of Formulation 3 cuvettes plotted together, with the one population standard deviation bands included to show the level of agreement between the two data sets. The average sensitivity for Groups 1 and 2 was  $0.0691 \pm 0.0023 \Delta\text{OD}/\text{Gy}$  and  $0.0691 \pm 0.0015 \Delta\text{OD}/\text{Gy}$ , respectively, with the uncertainty values representing one population standard deviation. Thus, all measured sensitivities were within two population standard deviations of the average.

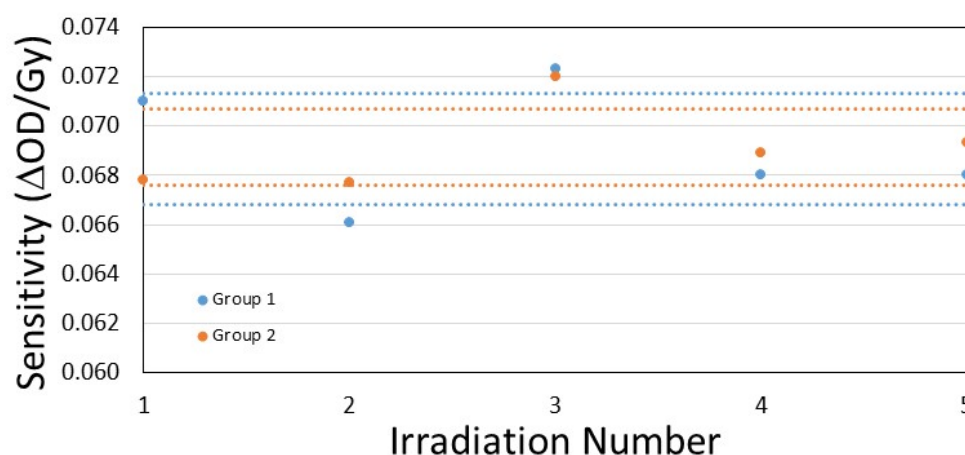


**Figure 10.** The measured sensitivity for each of the five irradiations of both Formulation 3 groups is plotted above. The dotted lines represent the one population standard deviation bounds from the average for each group.

## 4. Discussion

### 4.1. Linearity of Initial OD Response

The OD response to irradiation for all three formulations displays a linear relationship (Figure 3) with R<sup>2</sup> coefficients ranging from 0.9966 to 0.9997. The linearity of response to radiation suggests that all three formulations are viable candidates for use as a dosimeter for at least a single irradiation.

### 4.2. Initial Clearing Behavior

The OD clearing curves for the three formulations have significantly different decay times. Formulation 1 (Figure 4) required around twelve days to decay back to 1% of the post-irradiation OD. Formulation 2 (Figure 5) did not clear after two weeks. The decay curves for Formulation 3 (Figure 6) show the shortest time constant, and this formulation clears back to 1% of post-irradiation OD in around seven days. Thus, one could re-irradiate Formulations 1 and 3 after approximately twelve and seven days, respectively, but will have to wait longer if irradiating to higher doses than presented here. Due to the incomplete clearing of Formulation 2, it was not considered a viable reusable formulation (it reached a stable baseline after several weeks). The equilibrium (Figure 1) between the LMG and MG radical can explain these various clearing characteristics. Formulations 1 and 2, from a mechanistic point, have additional structurally hindering chemical interaction with the

methine carbon since they have more additional substituents than LMG in Formulation 3; consequently, the methine carbon is more readily reduced back to LMG by HBr, resulting in faster clearance times.

#### 4.3. Reusability and Dose Sensitivity upon Reirradiation

Subsequent re-irradiations of Formulations 1 and 3 (in duplicate) show that the OD cleared more rapidly than their respective initial irradiations, consistent with previously reported PRESAGE reusability studies [9]. The clearing times for Formulation 1 dropped to around seven days, while the clearing time for Formulation 3 dropped to less than 50 h.

Figure 7 and Table 2 show that the calibration curve slope decreases upon reirradiation of Formulation 1, displaying a decrease in sensitivity after each subsequent irradiation. For example, the second and third irradiations showed significant drops in sensitivity (24% and 40%, respectively) from the initial irradiation. Still, the subsequent irradiations showed much more minor changes from the previous irradiation. In other words, the dose sensitivity decreases upon reirradiation, while the linearity is maintained with mean absolute percentage errors (MAPE) (Table 3) ranging from 1.2% to 4.5%.

Similarly, the linearity of Formulation 3 (Figures 8 and 9, and Table 4) is maintained but differs significantly from Formulation 1 in that the dose sensitivity is much more consistent upon reirradiation. Figure 10 shows that the average sensitivity for both Group 1 and Group 2 agreed with a population standard deviation of 3.3% and 2.3%, respectively. Indicating that the sensitivity remains consistent upon reirradiation of Formulation 3 while also retaining linearity of response with MAPE values (Table 5) ranging from 1.8% to 4.7%.

Both Formulations 1 and 3 have linear dose-response over the same dose range. However, Formulation 1 drops significantly after the first irradiation, while Formulation 3 retains response sensitivity upon reirradiation, with no systematic decrease in sensitivity observed. With varying results on the behavior of the sensor response upon subsequent irradiations for Formulation 1, it will not be possible to perform absolute dosimetry measurements with this formulation without requiring a new sensitivity measurement to be performed each time. Since Formulation 1 does, however, retain linearity with each subsequent irradiation, it is possible to perform accurate relative dosimetry measurements with dosimeters manufactured using this formulation. Formulation 3 is the most reusable since it retains linearity and sensitivity of response upon reirradiation. Therefore, it may be possible to manufacture reusable 3D dosimeters for absolute dosimetry with this formulation, certainly for relative dosimetry measurements.

Both Formulations 1 and 3 show a decrease in clearing time upon reirradiation, with cuvettes in the present work stored at room temperature. PRESAGE samples stored in colder environments, such as refrigerated (4 °C) or freezing (−18 °C), exhibit greater stability in their temporal response and thus can be measured at later elapsed times post-irradiation while preserving their signal and maintaining a high degree of linearity [12]. Another factor influencing decay time is the dosimeter size, where scaling up from a small dosimeter cuvette to a larger 1 kg dosimeter has seen decay rates decrease by 3× [9].

**Author Contributions:** J.R.N.: Contribution Statement: The author made a substantial contribution to experimental design, drafting the article, data collection, analysis and interpretation, and final approval of the submitted article. M.R.: Contribution Statement: The author substantially contributed to data collection, analysis, experimental design, and article editing. J.A.H.: Contribution Statement: The author participated in data collection, dosimetric calculations, experimental design, editing the article, and final approval of the version to be submitted. G.S.: Contribution Statement: The author contributed to the article's data collection and analysis and editing. C.I.: Contribution Statement: The author contributed to data collection and analysis and editing the article. P.A.R.: Contribution Statement: The author contributed to data collection and analysis and editing the article. J.A.: Contribution Statement: The author made a substantial contribution to drafting the article and final approval of the version to be submitted, along with the creation of dosimeters for this work. All authors have read and agreed to the published version of the manuscript.

**Funding:** This research received no external funding.

**Conflicts of Interest:** John Adamovics is a Professor at Rider University and has a financial interest in Heuris Inc., which provided the dosimeters used in this research.

## References

1. Kry, S.F.; Alvarez, P.; Cygler, J.E.; DeWerd, L.A.; Howell, R.M.; Meeks, S.; O'Daniel, J.; Reft, C.; Sawakuchi, G.; Yukihiro, G.; et al. AAPM TG 191: Clinical use of luminescent dosimeters: TLDs and OSLDs. *Med. Phys.* **2019**, *47*, e19–e51. [[CrossRef](#)] [[PubMed](#)]
2. Yanagisawa, S.; Maruyama, D.; Oh, R.; Koba, Y.; Andoh, T.; Shinsho, K. Two-dimensional Thermoluminescence Dosimetry Using Al<sub>2</sub>O<sub>3</sub>: Cr Ceramics for 4, 6, and 10 MV X-ray Beams. *Sens. Mater.* **2020**, *32*, 1479. [[CrossRef](#)]
3. Niroomand-Rad, A.; Chiu-Tsao, S.; Grams, M.P.; Lewis, D.F.; Soares, C.G.; Van Battum, L.J.; Das, I.J.; Trichter, S.; Kissick, M.W.; Massillon-Jl, G.; et al. Report of AAPM Task Group 235 Radiochromic Film Dosimetry: An Update to TG-55. *Med Phys.* **2020**, *47*, 5986–6025. [[CrossRef](#)] [[PubMed](#)]
4. Oaki, Y.; Ishijima, Y.; Imai, H. Emergence of temperature-dependent and reversible color-changing properties by the stabilization of layered polydiacetylene through intercalation. *Polym. J.* **2018**, *50*, 319–326. [[CrossRef](#)]
5. Hall, A.V.; Musa, O.M.; Hood, D.K.; Apperley, D.C.; Yufit, D.S.; Steed, J.W. Alkali Metal Salts of 10,12-Pentacosadiynoic Acid and Their Dosimetry Applications. *Cryst. Growth Des.* **2021**, *21*, 2416–2422. [[CrossRef](#)] [[PubMed](#)]
6. Collins, C.; Yoon, S.W.; Kodra, J.; Coakley, R.; Subashi, E.; Sidhu, K.; Adamovics, J.; Oldham, M. An investigation of a novel reusable radiochromic sheet for 2D dose measurement. *Med Phys.* **2019**, *46*, 5758–5769. [[CrossRef](#)] [[PubMed](#)]
7. Khezerloo, D.; Nedaie, H.A.; Takavar, A. PRESAGE<sup>®</sup> as a solid 3D dosimeter: A review article. *Radiat. Phys. Chem.* **2017**, *141*, 88–97. [[CrossRef](#)]
8. Oldham, M. Methods and techniques for comprehensive 3D dosimetry. In *Advances in Medical Physics*; Godfrey, D., Das, S., Wolbars, A., Eds.; Medical Physics Pub Corp: Madison, WI, USA, 2014; pp. 70–81.
9. Juang, T. Clinical and Research Applications of 3D Dosimetry. PhD Thesis, Duke University, Durham, NC, USA, 2015. Available online: <https://dukespace.lib.duke.edu/dspace/handle/10161/10478> (accessed on 10 January 2021).
10. Adamovics, J.A. Detection of therapeutic radiation in three-dimensions. *Beilstein J. Org. Chem.* **2017**, *13*, 1325–1331. [[CrossRef](#)] [[PubMed](#)]
11. Adamovics, J.; Coakley, R. Chemical Dosimeters. In *Journal of Physics: Conference Series*; IOP Publishing: Bristol, UK, 2019; p. 012028.
12. Liu, K.; Wang, Y.; Lemus, O.M.D.; Adamovics, J.; Wu, C. Temperature dependence and temporal stability of stacked radiochromic sheets for three-dimensional dose verification. *Med. Phys.* **2020**, *47*, 5906–5918. [[CrossRef](#)] [[PubMed](#)]